Available online at www.sciencedirect.com
ScienceDirect
Journal of Sound and Vibration 322 (2009) 532–553
JOURNAL OF SOUND AND VIBRATION
www.elsevier.com/locate/jsvi

Dynamical chaos for a limited power supply for fluid oscillations in cylindrical tanks

T.S. Krasnopolskaya[a,*], A.Yu. Shvets[b]

[a]*Institute of Hydromechanics of the National Academy of Sciences, str. Zheljabova, 8/4, 03057 Kiev, Ukraine*
[b]*NTUU Kiev Polytechnic Institute, pr. Pobedy, 37, 03057 Kiev, Ukraine*

Accepted 4 September 2008
The peer review of this article was organised by the Guest Editor
Available online 19 October 2008

Abstract

Forced oscillations of the fluid surface in a cylindrical tank due to interaction with the excitation mechanism of a limited power supply (so-called "limited excitation" phenomena) are investigated in detail. On the basis of analysis of the largest Lyapunov exponents for a complex system—a tank with fluid and an excitation arrangement—the three types of steady-state regimes are found: equilibrium positions, periodic and chaotic regimes. Phase portraits, Poincaré sections and maps, distributions of spectral densities and invariant measures are constructed and thoroughly studied. Attention is concentrated mainly on the properties of chaotic attractors and schemes of transition from "order" to chaos. It is established that different scenarios of transition to chaos and various structures of chaotic attractors are possible in the same physical system. The new scenario transition to chaos which generalizes scenario of Pomeau–Manneville is revealed. It is shown that chaotic regimes with the single-mode fluid free surface oscillations can originate only due to interaction with the excitation mechanism.

1. Introduction

Possible modes of fluid free surface oscillations in a rigid container have been studied intensively from different points of view. The revolution in our understanding of the physics of the phenomenon brought about by the discovery of chaotic types of motion in deterministic systems has forced reevaluation of previous results, in particular, the details of chaotic types of motion in certain physical systems. In addition, the discovery of chaos has changed the methodology used to study these problems; it has broken down earlier stereotypes, and has led to the rejection of certain unfounded assumptions, such as the method of reduction, which states that the behavior of a complicated system can be determined by the properties of its component sub-systems. The new point of view is that the dynamics of a complicated system depends very much on the coupling between the sub-systems. For example, in cases where certain normal modes of vibration of a distributed system are coupled and have the same frequency, regular steady-state vibrations

*Corresponding author. Tel.: +380 44 456 9705; fax: +380 44 455 6432.
E-mail addresses: t.krasnopolskaya@tue.nl (T.S. Krasnopolskaya), alex.shvets@bigmir.net (A.Yu. Shvets).

0022-460X/$ - see front matter © 2008 Elsevier Ltd. All rights reserved.
doi:10.1016/j.jsv.2008.09.007

of any of the modes will "deteriorate" into chaotic motion because of the nonlinear interaction between them [1–5].

Another example of such coupling is the interaction of a vibrating system with an excitation mechanism. This interaction always exists because of the law of conservation of energy. When the vibrating system possesses damping (actually damping is present in all real systems), the dissipation of the energy could introduce essential corrections into the regimes of mechanism functioning. In this way, the vibrating system influences the parameters of the excitation force. This influence is considered significant when the power of the excitation mechanism is comparable to the power dissipated in the vibrating system. In this case the vibrating system has a limited (non-ideal) excitation and the mechanism has a limited power supply (or is non-ideal energy source), as was stated by Kononenko [6]. This situation is considered in the present study. The limited non-ideal excitation phenomena was first studied by Sommerfeld [7] and Timoshenko [8]. In these studies attention was focused on the changes of electric motor working regime, and not on the vibrating system. As shown by Kononenko [6], for a linear oscillator with limited excitation the characteristics of a nonlinear oscillator arise, such as the occurrence of instability regions. In view of this, in the present study, the existence of new possible characteristics is investigated for forced resonant oscillations of the fluid in tanks, which result from the interaction of the vibrating system with the energy source—the electromotor (electric motor).

2. Formulation of the problem

Suppose that the electric motor D is connected by a crank connecting-rod mechanism with a rigid cylindrical tank partly filled with a fluid (Fig. 1). The rotation of the electric motor shaft is described by the law of the change of angle $\Theta(t)$. When the crank a turns by the angle Θ, the tank is displaced in the space $u(t) = a\cos\Theta(t)$, which contains components along the axes O^*z^* and O^*y^* of the absolute coordinate system. These components are equal to $u_z = a\cos\Theta_0^*\cos\Theta(t)$ and $u_x = a\sin\Theta_0^*\cos\Theta(t)$, respectively, where Θ_0^* is the three-dimensional angle formed by the plane of tank platform and the horizontal plane $y^*O^*z^*$. The axis of the electric motor shaft is assumed to be parallel to the axis O^*y^*. For the description of the fluid free surface vibrations in the tank, we introduce the cylindrical coordinate system $Oxr\theta$, with origin on the undisturbed

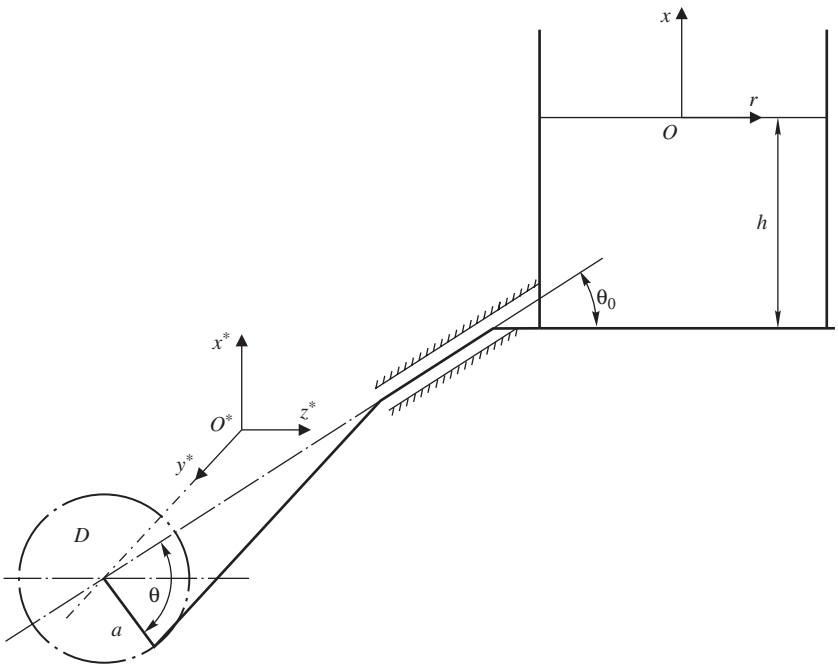

Fig. 1. Scheme of the system.

surface of the fluid. Then the equation of the fluid free surface may be written in the form

$$x = \eta(r, \theta, t). \tag{1}$$

Assuming that the fluid in the tank is inviscid and incompressible, and the induced motion is irrotational, the velocity field can be presented using velocity potential $\varphi(\eta, r, \theta, t)$, for which the mathematical boundary problem can be formulated in the form [1,2,9,10]:

$$\nabla^2\varphi = 0 \quad (-h < x < \eta; r, \theta \in S),$$

$$\left.\frac{\partial\varphi}{\partial r}\right|_{r=0} < \infty, \quad \left.\frac{\partial\varphi}{\partial r}\right|_{r=R} = 0, \quad \left.\frac{\partial\varphi}{\partial x}\right|_{x=-h} = 0,$$

$$\frac{\partial\varphi}{\partial x} - \nabla\eta\nabla\varphi = \left.\frac{\partial\eta}{\partial t}\right|_{x=\eta}. \tag{2}$$

Eq. (2) and boundary conditions can be obtained from the requirement of constancy of the integral over the volume Q and the cross-sectional surface S of the fluid

$$SI_1 = \frac{1}{2}\int\int_Q\int(\nabla\varphi^2)\,\mathrm{d}S\,\mathrm{d}x - \int_S\int(\varphi)|_{x=\eta}\frac{\partial\eta}{\partial t}\,\mathrm{d}S \tag{3}$$

under variations $\delta\varphi$ (Hamilton's principal). Then solutions of the problem $\eta(r, \theta, t)$ and $\varphi(x, r, \theta, t)$ can be written as series of eigenmodes [1,11]

$$\eta(r,\theta,t) = \sum_{ij}\left[\eta^c_{ij}(t)\frac{J_i\left(\frac{\mu_{ij}r}{R}\right)}{N_{ij}}\cos\mathrm{i}\theta + \eta^s_{ij}(t)\frac{J_i\left(\frac{\mu_{ij}r}{R}\right)}{N_{ij}}\sin\mathrm{i}\theta\right],$$

$$\varphi(x,r,\theta,t) = \sum_{ij}[\varphi^c_{ij}(t)X_{ij}(x,r)\cos\mathrm{i}\theta + \varphi^s_{ij}(t)X_{ij}(x,r)\sin\mathrm{i}\theta], \tag{4}$$

where $\eta^c_{ij}(t)$, $\eta^s_{ij}(t)$ and $\varphi^c_{ij}(t)$, $\varphi^s_{ij}(t)$ are unknown amplitudes of eigenmodes; $J_i(\mu_{ij}r/R)N^{-1}_{ij}\cos\mathrm{i}\theta$, $J_i(\mu_{ij}r/R)N^{-1}_{ij}\sin\mathrm{i}\theta$, $X_{ij}\cos\mathrm{i}\theta$, $X_{ij}\sin\mathrm{i}\theta$ are members of the complete set of orthogonal eigenfunctions.

$$X_{ij}(x,r) = \operatorname{sech}\left(\frac{\mu_{ij}}{R}h\right)\operatorname{ch}\left[\frac{\mu_{ij}}{R}(h+x)\right]\frac{J_i\left(\frac{\mu_{ij}}{R}r\right)}{N_{ij}},$$

$$N^2_{ij} = \frac{1}{2}(1+\delta_{0i})\left[1-\left(\frac{i}{\mu_{ij}}\right)^2\right]J_i(\mu_{ij}), \quad i = 0,1,2,\ldots,\ j = 1,2,3,\ldots\ . \tag{5}$$

Here $J_i(.)$ are Bessel functions; μ_{ij} are eigenvalues determined by $J'_i(\mu_{ij}) = 0$; δ_{ij} is the Kronecker delta.

We follow the notation of Miles [1,11], according to which the Lagrangian L could be written constructing kinetic and potential energies in the form [5,9,10] (here and in the following the summation is carried out for values with identical indices):

$$L = \frac{1}{2}I\dot{\Theta}^2 + \frac{1}{2}m_0a^2\dot{\Theta}^2\sin\Theta(t) + \frac{1}{2}\rho S\sum a^{c,s}_{ijmn}\dot{\eta}^{c,s}_{ij}\dot{\eta}^{c,s}_{mn} - \frac{1}{2}\rho S\sum[(g+\ddot{u}_x)\eta^{c,s}_{ij}\eta^{c,s}_{ij} - \ddot{u}_zQ_{1j}\eta^c_{1j}], \tag{6}$$

where I is the moment of inertia of the electric motor shaft [6], m_0 is the mass of the tank filled with fluid, ρ is the density of the fluid, S is the cross-sectional area of the circular cylindrical tank, $a^{c,s}_{ijmn} = a^{c,s}_{ijmn}(\eta^{c,s}_{ij}, \eta^{c,s}_{mn})$ are nonlinear functions of the unknown variables $\eta^{c,s}_{ij}$ (for more details see Refs. [1,11]), $Q_{1j} = (1/SN_{1j})\int\int r\cos^2\theta J_1(\mu_{1\,j}r/R)r\,\mathrm{d}r\,\mathrm{d}\theta$, g is the acceleration of gravity, $\ddot{u}_x$ and $\ddot{u}_z$ are the vertical and horizontal acceleration, respectively, of the tank. The first two terms in Eq. (6) denote the kinetic energy of the electric motor shaft and of the tank with fluid as a whole.

Since the power of the electric motor which excites three-dimensional vibrations of the tank is comparable to the power dissipated in the fluid at vibrations with internal damping, so that the change of fluid vibratory

regime has a feedback influence on the process of formation of the excitation force. For these reasons, the rotation speed of the electric motor shaft $\dot{\Theta}(t)$ should not be considered as a prescribed value, as it depends not only on the characteristics of the electric motor, but also on the vibration of the fluid [5].

Using expressions for accelerations $\ddot{u}_x$ and $\ddot{u}_z$ in L, we obtain

$$L = \frac{1}{2}I\dot{\Theta}^2 + \frac{1}{2}m_0a^2\dot{\Theta}^2\sin^2\Theta(t) + \frac{\rho S}{2}\sum a^{c,s}_{ijmn}\dot{\eta}^{c,s}_{ij}\dot{\eta}^{c,s}_{mn} + a\rho S\cos\Theta_0(\dot{\Theta}^2\cos\Theta + \ddot{\Theta}\sin\Theta)\sum Q_{1j}\eta^{c,s}_{1j} + \frac{\rho S}{2}[a\sin\Theta_0(\dot{\Theta}^2\cos\Theta + \ddot{\Theta}\sin\Theta) - g]\sum \eta^{c,s}_{ij}\eta^{c,s}_{ij}. \quad (7)$$

On the basis of Eq. (7) we can easily construct the equations of Lagrange for the generalized coordinates of the electric motor, i.e., for the angle $\Theta(t)$ as

$$\begin{aligned} I\ddot{\Theta} = & -m_0a^2\sin\Theta\cos\Theta - m_0a^2\ddot{\Theta}\sin^2\Theta + a\rho S\cos\Theta_0(\Theta^2\sin\Theta \\ & - \ddot{\Theta}\cos\Theta)\sum Q_{1j}\eta^{c}_{1j} - 2a\rho S\dot{\Theta}\cos\Theta_0\cos\Theta\sum Q_{1j}\dot{\eta}^{c}_{1j} \\ & + a\rho S\sin\Theta_0(\Theta^2\sin\Theta - \ddot{\Theta}\cos\Theta)\sum \eta^{c,s}_{ij}\eta^{c,s}_{ij} - 4a\rho S(\sin\Theta_0)\dot{\Theta}\cos\Theta \\ & \times\sum \eta^{c,s}_{ij}\eta^{c,s}_{ij} + L(\dot{\Theta}) - H(\dot{\Theta}). \end{aligned} \quad (8)$$

The last two summations on the right-hand side of Eq. (8) are the driving torque and the torque of resistive forces of the electric motor [6]. The remaining terms on the right-hand side are torque of the reverse influence forces of vibrations of the fluid-filled tank and of the fluid free surface. The Lagrange equation for the unknown amplitudes $\eta^{c,s}_{ij}$ of eigenmodes may also be obtained from Eq. (7). In this case the problem is reduced to the analysis of infinite number of nonlinear mutually related equations relative to $\eta^{c,s}_{ij}$. This system has to be completed with the equation of energy source (8).

In the following we assume $\Theta^*_0 = 0$, which means that tank vibrations occur in the horizontal plane along the axis O^*z^*. Moreover we assume that the angular speed of the electric motor shaft $\dot{\Theta}(t)$ in the stationary regime is close to the eigenfrequency ω_{11} of the vibrations of the free surface of the first antisymmetric modes $\eta^c_{11}(t)N^{-1}_{11}J_1(k_{11}r)\cos\theta$ and $\eta^s_{11}(t)N^{-1}_{11}J_1(k_{11}r)\sin\theta$, where $k_{11} = \mu_{11}/R$. We introduce a small positive parameter

$$\varepsilon = (aQ_{11}k^2_{11})^{(1/3)}. \quad (9)$$

In this case the detuning of frequencies $\dot{\Theta}$ and ω_1 will be taken as a small value, proportional to ε^2, in the form [9,10]

$$\dot{\Theta}(t) - \omega_{11} = \tfrac{1}{2}\varepsilon^2\omega_{11}\beta(t), \quad (10)$$

where $\omega_{11} = (gk_{11}\tanh k_{11}h)^{1/2}$, h is the depth of the fluid in the tank; β is tuning parameter which measures the offset of frequency $\dot{\Theta}$ and ω_{11}. The vibrations of the free surface are approximated by dominant forms of vibrations [2] $\eta^c_{11}(t)N^{-1}_{11}J_1(k_{11}r)\cos\theta$ and $\eta^s_{11}(t)N^{-1}_{11}J_1(k_{11}r)\sin\theta$ as well as by secondary modes ($\eta^c_{21}(t)N^{-1}_{21}J_2(\mu_{21}r/R)\cos2\theta$, $\eta^s_{21}(t)N^{-1}_{21}J_2(\mu_{21}r/R)\sin2\theta$ and $\eta^c_{01}(t)N^{-1}_{01}J_0(\mu_{01}r/R)$), containing the harmonics $\cos2\theta, \sin2\theta$, $\cos0 \equiv 1$, as it was shown by Miles [1,2], that those modes have the biggest connection coefficients in equations for the dominant mode vibrations. We define functions $\eta^{c,s}_{ij}(t)$ in the form

$$\eta^c_{11} = \varepsilon\lambda[p_1(\tau)\cos\Theta(t) + q_1(\tau)\sin\Theta(t)],$$

$$\eta^s_{11} = \varepsilon\lambda[p_2(\tau)\cos\Theta(t) + q_2(\tau)\sin\Theta(t)] \quad (11)$$

for dominant modes and

$$\eta^{c,s}_{21} = \varepsilon\lambda[A^{c,s}_{21}(\tau)\cos2\Theta(t) + B^{c,s}_{21}(\tau)\sin2\Theta(t) + C^{c,s}_{21}(\tau)],$$

$$\eta^c_{01} = \varepsilon\lambda[A^c_{01}(\tau)\cos2\Theta(t) + B^c_{01}(\tau)\sin2\Theta(t) + C^c_{01}(\tau)], \quad (12)$$

for secondary modes, where $\lambda = k^{-1}_{11}\tanh(k_{11}h)$,

$$\tau = \tfrac{1}{2}\varepsilon^2\Theta(t) \quad (13)$$

is slow time; and the variables $p_1(\tau), q_1(\tau), p_2(\tau), q_2(\tau), A_{21}^{c,s}(\tau), B_{21}^{c,s}(\tau), C_{21}^{c,s}(\tau),\ A_{01}^{c}(\tau), B_{01}^{c}(\tau), C_{01}^{c}(\tau)$ are slowly varying dimensionless amplitudes of the dominant and the secondary modes.

Upon introducing Eqs. (11) and (12) into Eq. (7) and averaging L over the fast time $\Theta(t)$, an expression may be obtained for the averaged Lagrangian $\langle L\rangle$. After determination of $A_{21}^{c,s}(\tau), B_{21}^{c,s}(\tau), C_{21}^{c,s}(\tau),\ A_{01}^{c}(\tau), B_{01}^{c}(\tau)$, $C_{01}^{c}(\tau)$ and their introducing into $\langle L\rangle$ we finally find in the first approximation

$$\langle L\rangle = \frac{1}{2}I\dot{\Theta}^2 + \frac{1}{4}m_0a^2\dot{\Theta}^2 + \frac{1}{2}\varepsilon^4 g\lambda^2\rho S\left[\frac{1}{2}\sum\left(\frac{\mathrm{d}p_n}{\mathrm{d}\tau}q_n - p_n\frac{\mathrm{d}q_n}{\mathrm{d}\tau}\right) + p_1 + \frac{\ddot{\Theta}}{\omega_1^2}q_1 + \beta(\tau)E + \frac{1}{2}AE^2 + \frac{1}{2}BM^2\right], \tag{14}$$

where A, B—constant coefficients given in Miles work [1];

$$E = E_1 + E_2, \quad E_n = \tfrac{1}{2}(p_n^2 + q_n^2), \quad M = p_1q_2 - p_2q_1, \quad n = 1, 2.$$

E and M are the energy and the angular momentum, respectively, of the vibrations of the fluid in the fundamental modes.

Now we write the equations for p_i and q_i which follow from Eq. (14). We take into account the forces of viscous damping $\varepsilon^2\delta\dot{\eta}_{ij}^{c,s}$ [2,9–11]

$$\begin{aligned}
\frac{\mathrm{d}p_1}{\mathrm{d}\tau} &= \alpha p_1 - (\beta + AE)q_1 + BMp_2,\\
\frac{\mathrm{d}q_1}{\mathrm{d}\tau} &= \alpha q_1 + (\beta + AE)p_1 + BMq_2 + 1,\\
\frac{\mathrm{d}p_2}{\mathrm{d}\tau} &= \alpha p_2 - (\beta + AE)q_2 - BMp_1,\\
\frac{\mathrm{d}q_2}{\mathrm{d}\tau} &= \alpha q_2 + (\beta + AE)p_2 - BMq_1,
\end{aligned} \tag{15}$$

where $\alpha = -\delta/\omega_{11}$, δ is the damping ratio, when $2\pi\delta$ is the logarithmic decrement which may be obtained either by direct measurement of the decay of the dominant modes or through semiempirical calculation [2].

In problems of an ideal excitation of vibrations of the fluid free surface (when the power of excitation mechanism is infinite and the feedback of the vibrating system on this mechanism may be neglected) the system of equations (15) would have been a four-parametric one. However, in the formulation of the problem considered in this paper, when the excitation unit-electric motor is "sensitive" to the level of energy dissipation by the vibrating system, we must consider $\beta(\tau)$ Eq. (10) not as a constant coefficient, but as an additional unknown. Since the value $\Theta(t)$ depends on vibrations of the liquid, the value of frequencies difference $\beta(\tau)$ will be determined by the whole history of interaction between the rotation of an electric motor shaft and the vibrations of the fluid free surface. In order to close system (15) we need an equation for β. We proceed in the following manner: we introduce a change of variables, as is usual in problems of limited excitation

$$\dot{\Theta}(t) = \Omega(\tau). \tag{16}$$

Then from Eqs. (11) and (12) by averaging over the fast time $\Theta(t)$ we can write Eq. (8) in the following form ($\Theta_0^* = 0$):

$$\frac{\mathrm{d}\Omega}{\mathrm{d}t} = \varepsilon^4\left[M_1(\Omega) - \alpha_1\lambda\Omega^2q_1 - \alpha_1\lambda\frac{\mathrm{d}\Omega}{\mathrm{d}t}p_1\right] + \varepsilon^5\ldots. \tag{17}$$

Here

$$\varepsilon^4 M_1(\Omega) = \frac{\Phi(\Omega) - H(\Omega)}{I + 0.5m_0a^2}, \quad \varepsilon^3\alpha_1 = \frac{aQ_1\rho S}{2I + m_0a^2}.$$

In the slow time we have

$$\frac{d\Omega}{d\tau} = \varepsilon^2 M_2(\Omega) - \varepsilon^2 \mu q_1, \tag{18}$$

when

$$\varepsilon^2 M_2(\Omega) = \frac{2\varepsilon^2}{\omega_1} M_1, \quad \mu = 2\lambda\alpha_1\omega_1.$$

As we are interested in the steady-state response, the static characteristic of $\Phi(\Omega)$ of the electric motor [6] will be used. Accordingly, we assume $\varepsilon^2 M_2(\Omega) = \varepsilon^2(N_0 + N_1\Omega)$; N_0, N_1 are constants.

Moreover, we transform Eq. (18) into equation for $\beta(\tau)$

$$\frac{d\beta}{d\tau} = N_3 + N_1\beta - \mu_1 q_1, \tag{19}$$

where

$$N_3 = \frac{2}{\omega_1}(N_0 + N_1\omega_1), \quad \mu_1 = \frac{2\mu}{\omega_1}.$$

Consequently, we conclude that the process of interaction between vibrations of the fluid free surface in dominant resonant modes and the shaft rotation of the electric motor with limited power supply is described by a system of five evolution equations [9,10]

$$\begin{aligned}
\frac{dp_1}{d\tau} &= \alpha_1 p_1 - (\beta + AE)q_1 + BMp_2,\\
\frac{dq_1}{d\tau} &= \alpha_1 q_1 + (\beta + AE)p_1 + BMq_2 + 1,\\
\frac{dp_2}{d\tau} &= \alpha_1 p_2 - (\beta + AE)q_2 - BMp_1,\\
\frac{dq_2}{d\tau} &= \alpha_1 q_2 + (\beta + AE)p_2 - BMq_1,\\
\frac{d\beta}{d\tau} &= N_3 + N_1\beta - \mu_1 q_1.
\end{aligned} \tag{20}$$

In the following we analyze the steady solutions of the system of equations (20), which may represent equilibrium states, periodic, almost-periodic and also chaotic solutions. In the five-dimensional phase-space $(p_1, q_1, p_2, q_2, \beta)$, these solutions correspond asymptotically to a point, a limit cycle, a limit torus, and a chaotic attractor, respectively. The condition for the occurrence of a chaotic attractor is the combination of total compression with local instability.

3. Steady-state trajectories

The system of equations (20) is nonlinear and analytical solutions are not found, numerical solutions were obtained. In the space of parameters $(\alpha, A, B, N_1, N_3, \mu_1)$ of the equations system (20) extensive numerical experiments were carried out in order to find the regions of existence of chaotic solutions and to investigate the transition from regular to chaotic regimes. The structural reorganization of phase portraits of the chaotic attractors was also investigated. The main computational method of the numerical integration of Eqs. (20) was a fifth-order Runge–Kuttas method with the correction of the variable computational interval according to Dormand–Prince [12]. A local numerical error of $O(10^{-12})$ or less was ensured. The construction of corresponding Poincaré cross-sections and maps of phase portraits for the steady-state solutions was carried out by the method of Henon [13]. In the case of chaotic vibrations the number of points in those cross-sections was about 10^4–10^5. The Lyapunov exponents were computed using Bennettin's method [14,15]. At last, for

construction of natural invariant measures, the technique of coding by nuances of black color [5] is applied. In order to minimize the effect of transients, all the temporal realizations of the dynamic processes were analyzed after a prolonged time interval. The system of equations (20) has six parameters $(\alpha, A, B, N_1, N_3, \mu_1)$ which together with the initial conditions determine its behavior in the steady regimes. We may remark, that some from these parameters are multiparameters. We shall define the type of the given set of equations. With this purpose we find a divergence Δ systems (20). It is obvious that the divergence of a system can be written in the form:

$$\Delta \equiv \frac{\partial\left(\frac{dp_1}{d\tau}\right)}{\partial p_1} + \frac{\partial\left(\frac{dq_1}{d\tau}\right)}{\partial q_1} + \frac{\partial\left(\frac{d\beta}{d\tau}\right)}{\partial \beta} + \frac{\partial\left(\frac{dp_2}{d\tau}\right)}{\partial p_2} + \frac{\partial\left(\frac{dq_2}{d\tau}\right)}{\partial q_2} = 4\alpha + N_1. \tag{21}$$

Apparently from Eq. (21), the divergence of a system depends on viscous dampings coefficient α and parameter N_1 which characterize an angle of inclination static characteristics of the electromotor [6]. For real physical systems these parameters are always negative ones. Hence, the set of Eqs. (20) is dissipative. It means that any initial phase volume of the system aspires to zero at unlimited increase of time. That is, any initial subset of figuring points which has the non-zero phase volume eventually concentrates on one or several attractors, and these attractors have zero phase volume. As we shall see further, attractors in systems (20) can be regular and chaotic.

Let us consider bifurcations happening in the system when some of its parameters are changing. We assume that the tank is filled by a fluid up to the depth $h > 3R$, therefore, as shown in the work [1]:

$$A = 1.112, \quad B = -1.531. \tag{22}$$

The parameter of damping α is considered to be the small one [2]:

$$\alpha = -0.1. \tag{23}$$

Also we shall assume, that a requirement for preresonance interaction between the fluid free surface oscillations and the electromotor are realized, that is $N_3 < 0$. So, it is possible to accept that [6]

$$N_3 = -0.1, \quad \mu_1 = 0.5. \tag{24}$$

Initial conditions varied in a neighborhood of an origin of phase space coordinates of system (20). In particular, the selected initial conditions correspond to zero initial vibration amplitudes on the first dominant mode and to non-zero initial vibration amplitudes on a second dominant mode. For example

$$p_1(0) = 0, \quad q_1(0) = 0, \quad \beta(0) = 0, \quad p_2(0) = 1, \quad q_2(0) = 1.$$

First, we shall consider parameter N_1 as a bifurcation one. This parameter characterizes an angle of static characteristic inclination of the excitation engine.

As is known, the basic practical criterion of existence of a chaotic attractor in the system is the presence of at least one positive characteristic exponent in a spectrum of Lyapunov characteristic exponents. In Fig. 2 dependence of the maximum Lyapunov characteristic exponent λ_1 on value N_1 is shown. As it can be seen, intervals of parameter N_1 values exist in which the value λ_1 is positive. Hence, in these intervals the dynamic system (20) has chaotic attractors.

Let us consider in more detail transition from the regular attractors of system (20) to chaotic. As the carried out numerical calculations have shown at $-0.1 < N_1 \leqslant -0.05$ stable equilibrium positions exist with coordinates:

$$p_1 = \text{const.}, \quad q_1 = \text{const.}, \quad \beta = \text{const.}, \quad p_2 = q_2 = 0. \tag{25}$$

Thus, all stable equilibrium positions in the vicinity of the origin of phase space coordinates O at $-0.1 < N_1 \leqslant -0.05$ have zero coordinates of the second dominant mode. At $N_1 = -0.1$ this position of an

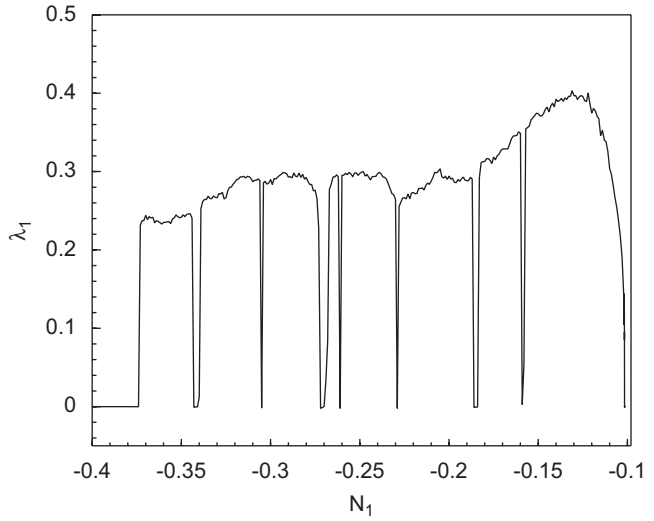

Fig. 2. Dependence of the maximum Lyapunov exponent λ_1 on parameter N_1.

equilibrium loses stability and a stable limit cycle with the zero second dominant mode originates in system (20) as a result of Andronov–Hopf bifurcation. That is, the limit cycle with

$$p_1 = f_1(\tau), \quad q_1 = f_2(\tau), \quad \beta = f_3(\tau), \quad p_2 = 0, \quad q_2 = 0,$$

where $f_1(\tau), f_2(\tau), f_3(\tau)$ are some periodic functions of τ.

Starting at the value $N_1 = -0.10153$ there is a cascade of period-doubling bifurcations of limit cycles. In Fig. 3 the first bifurcations of this cascade are shown. This infinite cascade of period-doubling bifurcations comes to the end by origin of a chaotic attractor at $N_1 = -0.101632$. In Fig. 4 projections of the chaotic attractor are given for $N_1 = -0.10164$. The projections shown in Fig. 4 correspond to chaotic oscillations only by the first dominant mode. Transition to chaos here happens under Feigenbaum scenario [16,17]. We should stress a very interesting feature that all bifurcations of the period-doubling cascade and the chaotic attractor have the zero second dominant mode of oscillations. Moreover, the chaotic attractor has spiral structure. Points on trajectories of the attractor unpredictable wander on coils of its spirals. In what follows, we shall name such attractors as single-mode ones.

In Fig. 4(c) the Poincaré section by the plane $\beta = -1.55$ is shown for the chaotic attractor at $N_1 = -0.10164$ and its Poincaré map on a variable q_1. Section of Poincaré represents the chaotic point set having a ribbon structure. Poincaré map can be exactly enough approximated by the one-dimensional curves. Thus, in this case investigation of the dynamic system (20) can be reduced to study the one-dimensional discrete map.

Let us remark that the period-doubling bifurcations happen on a very small length interval of changing N_1. However, the interval of existence of a single-mode chaotic attractor is smaller. So, at $N_1 = -0.10165$ the single-mode attractor disappears and in the system a chaotic attractor of another type appears. In Fig. 5 projections of the new chaotic attractor which arise in the system at $N_1 = -0.10165$ are given. First of all it differs from the single-mode attractor by excitation of oscillations on the second dominant mode. We name attractors of such type as double-mode ones. Besides, amplitudes of chaotic oscillations on the first dominant mode increase noticeably. Because of that the volume of a phase space, in which trajectories of arisen chaotic attractor are localized, increases. So, in Fig. 5 it is possible to notice a small densely blacked out area in the vicinity of the point $(1, 0)$. This blacked out area approximately corresponds to the area of localizations in the phase space of the missed single-mode attractor.

In Fig. 5(d) the enlarged fragment of the projection of the chaotic attractor in the vicinity of the point $(1, 0)$ is shown. A close study of this fragment allows to detect a noticeable likeness with the relevant projection of the single-mode attractor (Fig. 4(a)). It makes clear the mechanism of an origin of the double-mode chaotic attractor which is a result of an intermittency between the missed chaotic single-mode attractor and a saddle limit cycle existing near by in the phase space. At $N_1 = -0.10165$ the single-mode attractor and a saddle cycle

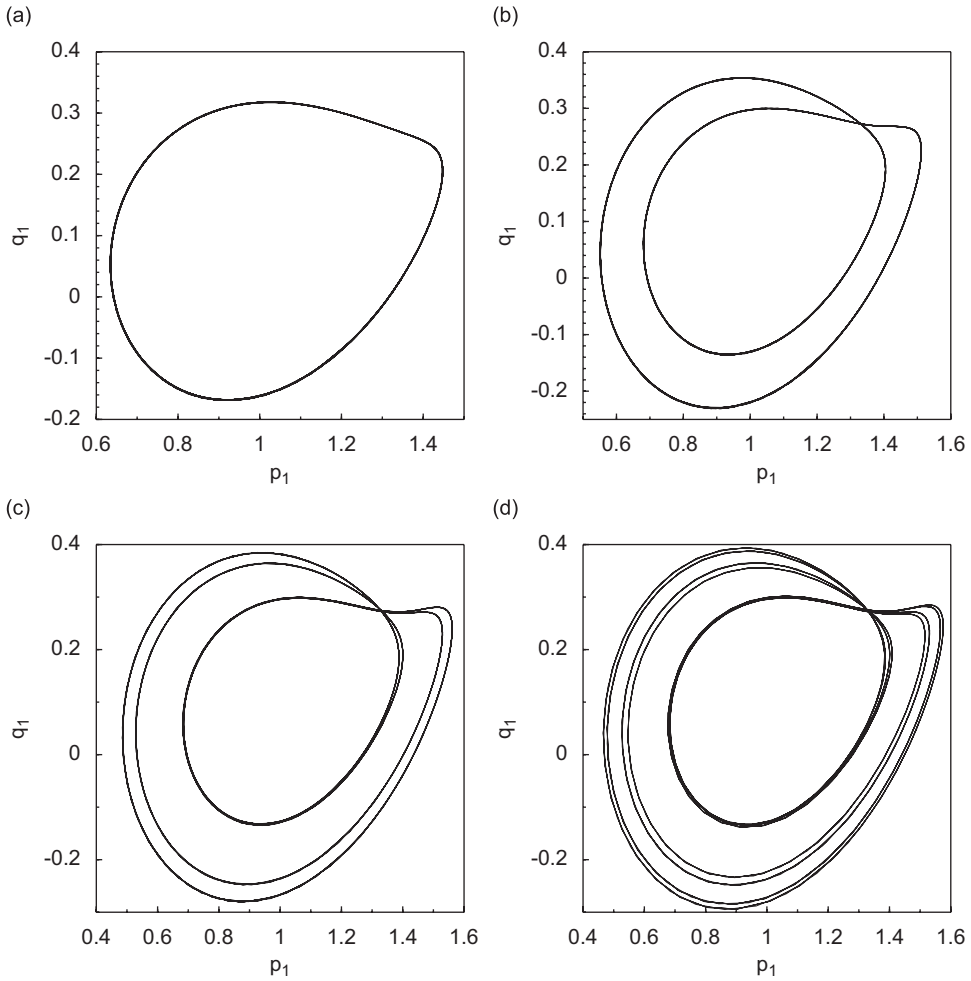

Fig. 3. Projections of the period—doubling bifurcation cascade: base cycle (a), first bifurcation (b), second bifurcation (c), third bifurcation (d).

disappear and in system (20) a new chaotic attractor appears. Motion along this attractor has three phases: laminar, turbulent and one, which we shall name as coarse grained laminar. Motion at the laminar phase corresponds to motion along the trajectories closely located to the missed limit cycle (see, densely retraced trajectories at the left above part in Fig. 5(a)). At unpredictable moments of time there is a turbulent splash (the turbulent phase) and trajectories go away to the area of the missed single-mode chaotic attractor (densely blacked out area in the vicinity of the point $(1,0)$ in Fig. 5(d). Then during maybe long time trajectories make chaotic wanderings along coils of the missed single-mode chaotic attractor. By analogy with the terminology used in the statistical physics [5,18–20] we name this phase as coarse grained laminar. In fact Gibbs in his classical textbook [18] introduced notion coarse grained density as the averaged characteristics in box (grains) when he studied processes statistically by box counting approach and not by continuum approach from point characteristics. Any process has the same characteristics in a box by coarse grained approach for all points. So if we look at the missed single-mode chaotic attractor using averaging procedure as modelling it in some boxes, then attractor may be presented as some limit cycle with one trajectory part in every box (not a lot of trajectory coils in every box) and with some jumps in coordinates of trajectories from one box to another. That is why we name motion along the missed single-mode chaotic attractor as coarse grained laminar phase and after the coarse grained laminar phase, in an unpredictable instant, new turbulent splash happens (the turbulent phase) and trajectories return in the area of the missed limit cycle. The described process iterates

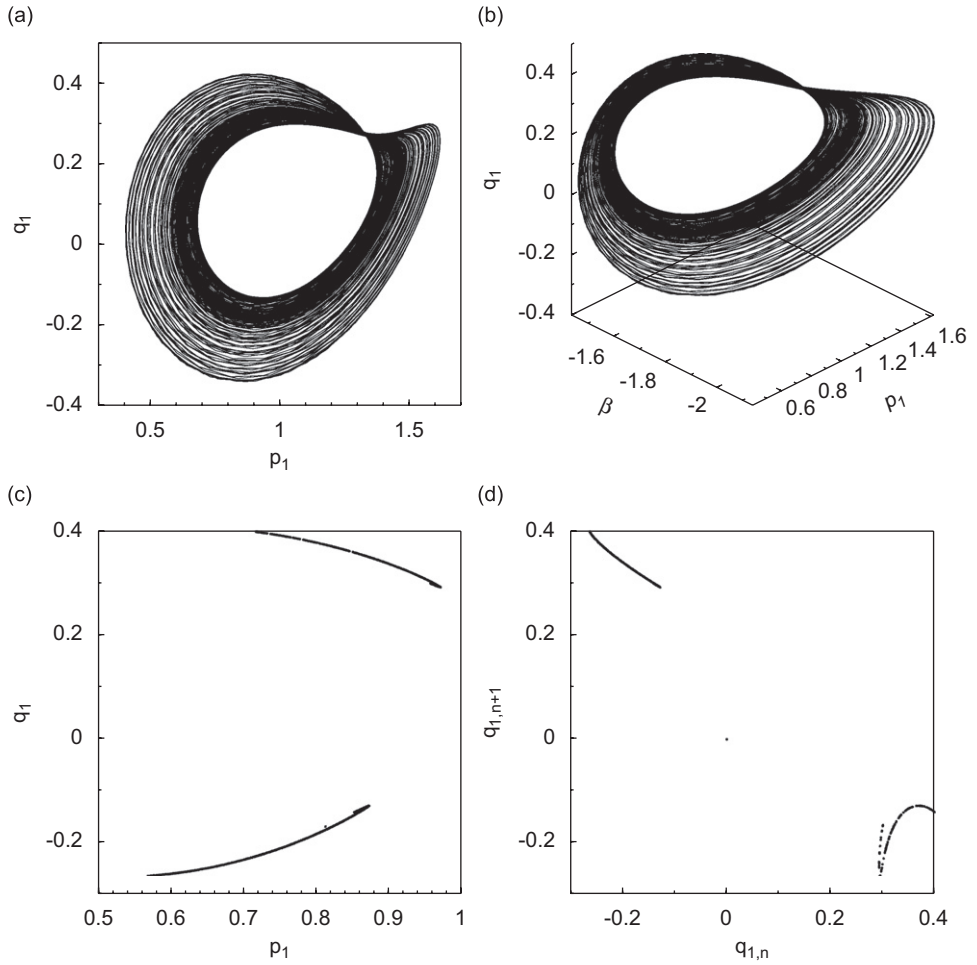

Fig. 4. Projections of a chaotic attractor at $N_1 = -0.10164$ (a,b), its Poincaré section (c) and map (d).

an infinite number of times. Thus, such intermittency is distinct from the classical type considered by Pomeau and Manneville [21–23], when there are only two phases in the intermittency: laminar and turbulent. We also want to point out that the double-mode chaotic attractor has more than triple growth in the value of the maximum Lyapunov characteristic exponent of system (20) from 0.023 up to 0.075.

In Fig. 6 projections of Poincaré section by a plane $\beta = -1.55$ and Poincaré map (of one of variables) of the double-mode chaotic attractor at $N_1 = -0.10165$ are given. Apparently the Poincaré section loses ribbon structure which existed in the single-mode attractor and looks as some developed chaotic point set. However, a close look at Fig. 6(a) allows to note that some constituent part of the double-mode chaotic attractor Poincaré section has a ribbon structure of the missed single-mode attractor. The same rule is proper also in Poincaré map of the double-mode attractor. The constituent part of this map is solid blacked "curves" which are as "memories" of the missed single-mode chaotic attractor. It is natural that for the double-mode chaotic attractor there is no one-dimensional discrete approximation.

We must admit that origin of the single-mode chaotic attractors is only due to interaction of oscillatory systems (fluid free surface) with the excitation engine–electric motor. At an unlimited power supply of the electric motor appearance of the chaotic single-mode regimes in system (20) is impossible.

The double-mode chaotic attractors exist on the much larger segment of the parameter N_1, namely $-0.373 \leqslant N_1 \leqslant -0.10165$. This segment corresponds to the area, in which system (20) has the positive maximum characteristic exponent, what is apparent from Fig. 2. However, in Fig. 2 number of touches of the characteristic exponent graph to a zero value is precisely seen. Small intervals, in which the characteristic

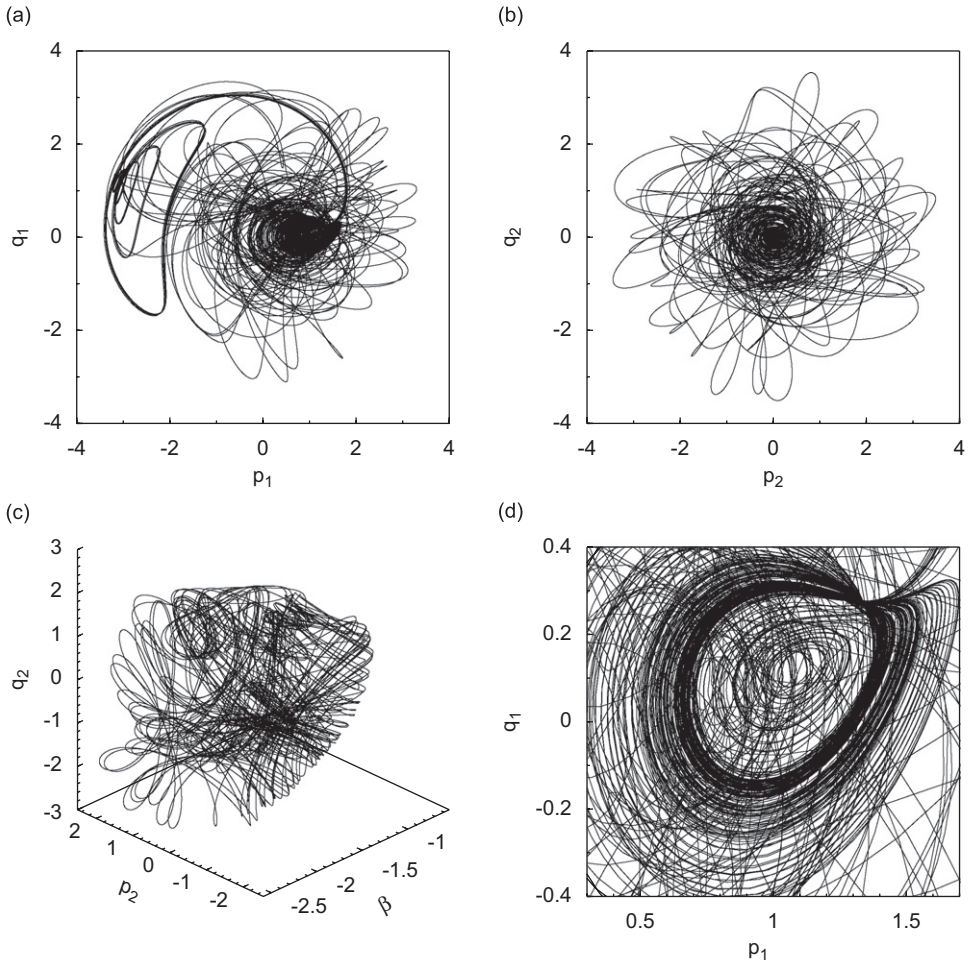

Fig. 5. Projections of the chaotic attractor at $N_1 = -0.10165$ (a–d).

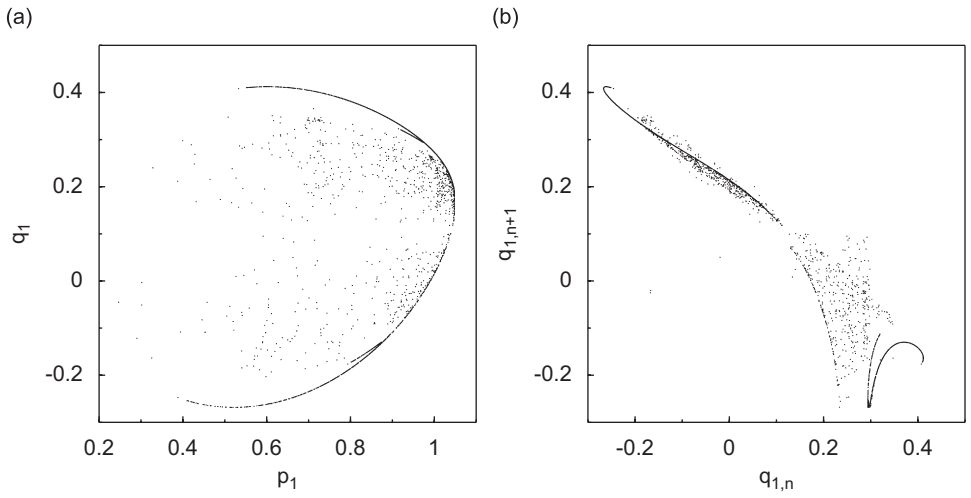

Fig. 6. Projections of Poincaré section (a) and map (b) of the chaotic attractor at $N_1 = -0.10165$.

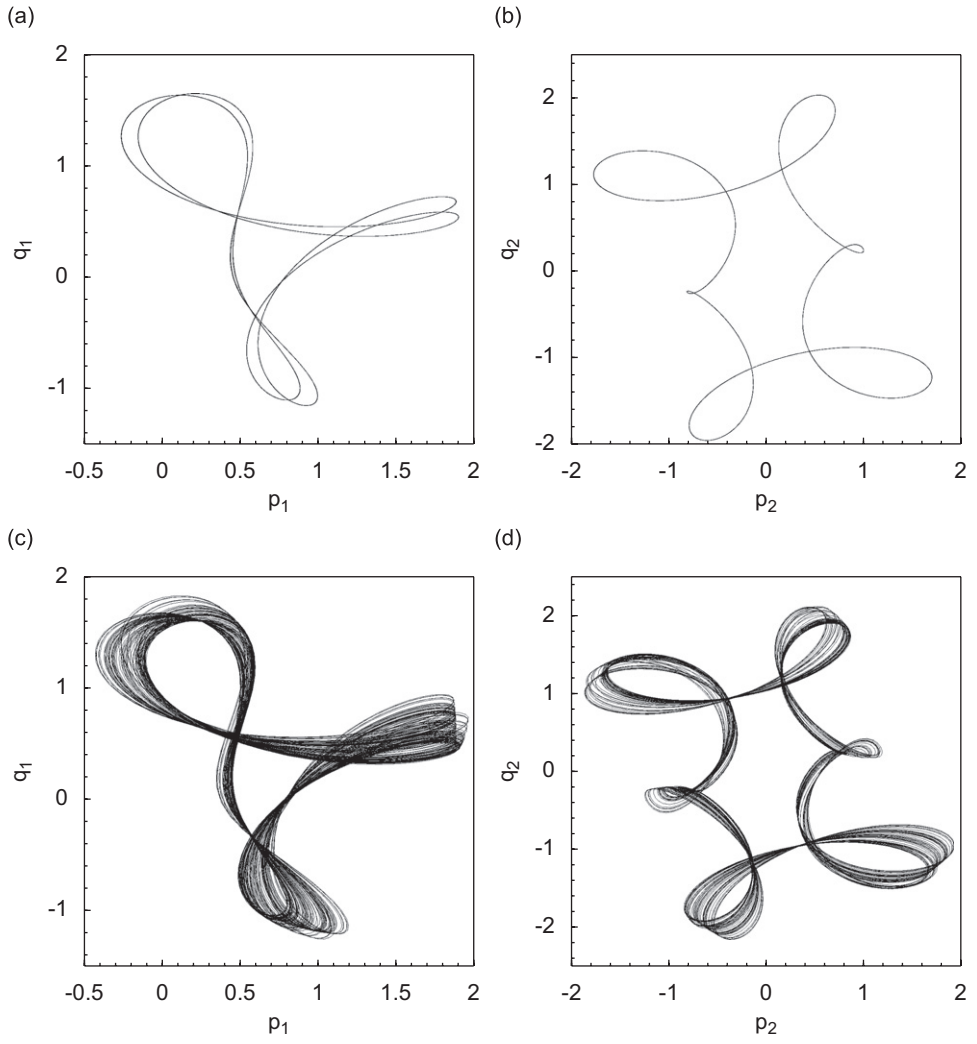

Fig. 7. Projections of a limit cycle at $N_1 = -0.271$ (a,b) and a chaotic attractor at $N_1 = -0.268$ (c,d).

exponent is equal to zero, correspond to ''windows of periodicity'' in the field of chaos. In these windows there are stable limit cycles in the system.

Let us consider the dynamics of system (20) at transition of one periodicity window. For example, at $N_1 = -0.271$ there is a limit cycle in the system, whose projections of the phase portrait are shown in Fig. 7(a) and (b). At $N_1 = -0.269$ the limit cycle disappears and as a result of the intermittency of the first type the chaotic attractor appears. Projections of the phase portrait of two modes of oscillations of such attractor constructed for $N_1 = -0.268$ are given in Fig. 7(c) and (d). In Fig. 8 projection of Poincaré section by the plane $\beta = -1.35$ and Poincaré map of the variable q_1 are presented. In spite of the fact that the arisen chaotic attractor is the double-mode one, projections of its Poincaré section have quasi-ribbon structure, more appropriate for the single-mode chaotic attractors. As is apparent from Fig. 8(b), it is possible to approximate the dynamics of the system by means of the discrete one-dimensional maps.

At increase in N_1 from the value -0.268 the double-mode chaotic attractor appears. In Fig. 9(a) and (b) two- and three-dimensional projections of the phase portrait of chaotic attractor at $N_1 = -0.25$ are shown. Accordingly in Fig. 9(c) and (d) its Poincaré section and map are demonstrated. The considerable changes and complicatedness of a phase portrait structure is obviously visible if we compare them to those which are for the chaotic attractor at $N_1 = -0.268$. Projections of Poincaré section (Fig. 9(c)) completely lose quasi-ribbon

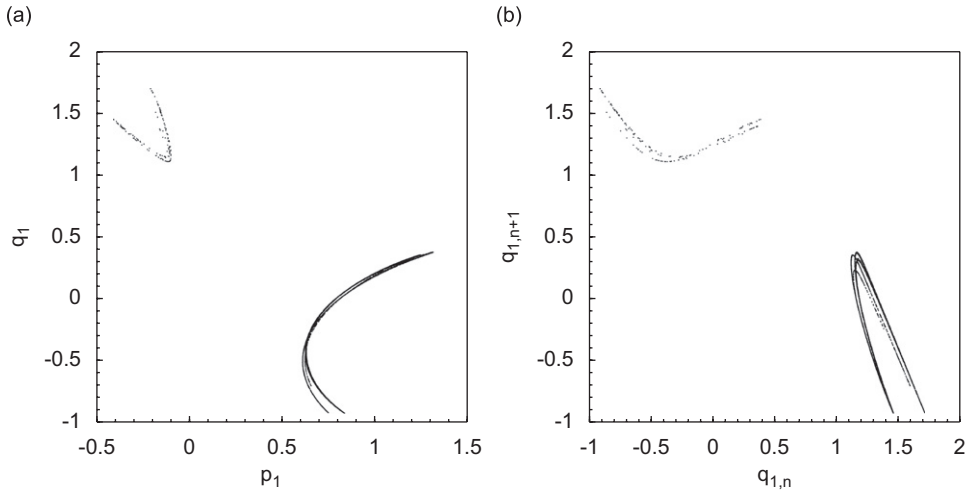

Fig. 8. Projections of Poincaré section by the plane $\beta = -1.35$ (a) and Poincaré map (b) of the chaotic attractor at $N_1 = -0.268$.

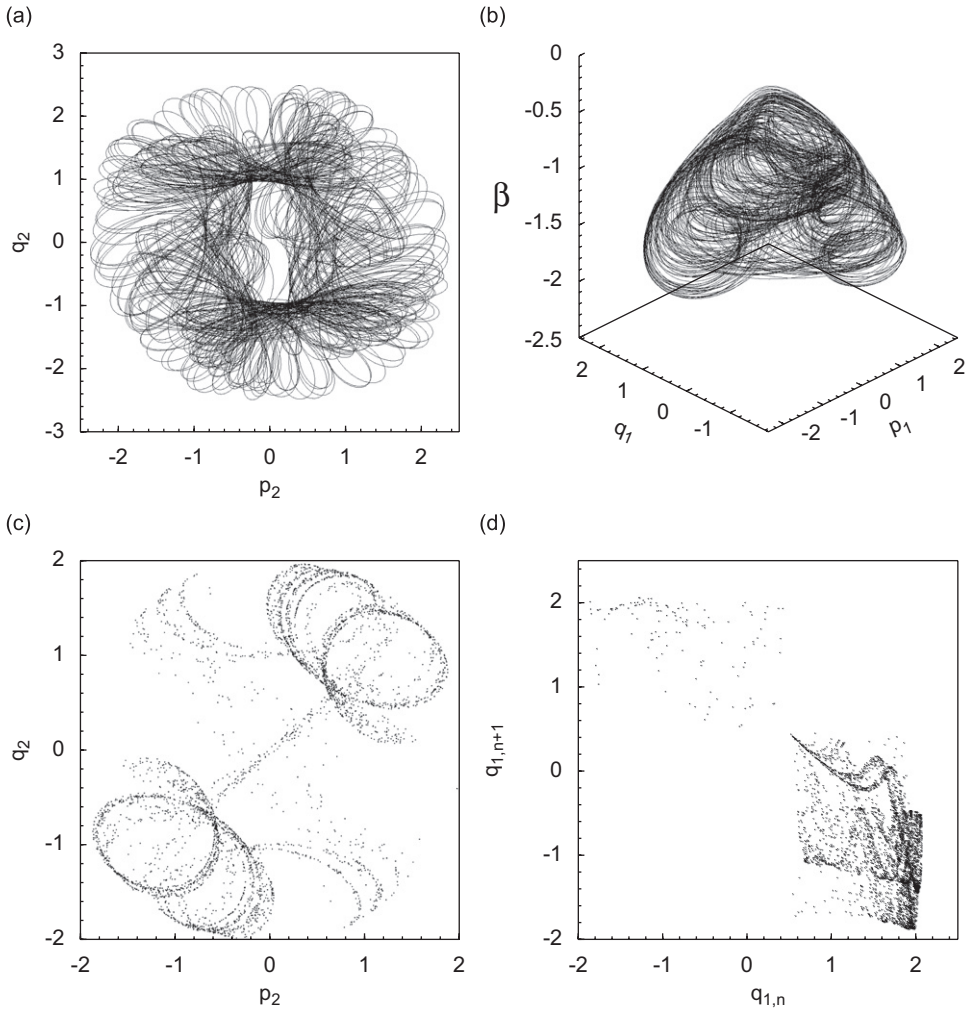

Fig. 9. Two- and three-dimensional projections of the phase portrait (a,b) and Poincaré section by the plane $\beta = -1.35$ (c) and Poincaré map (d) of a chaotic attractor at $N_1 = -0.25$.

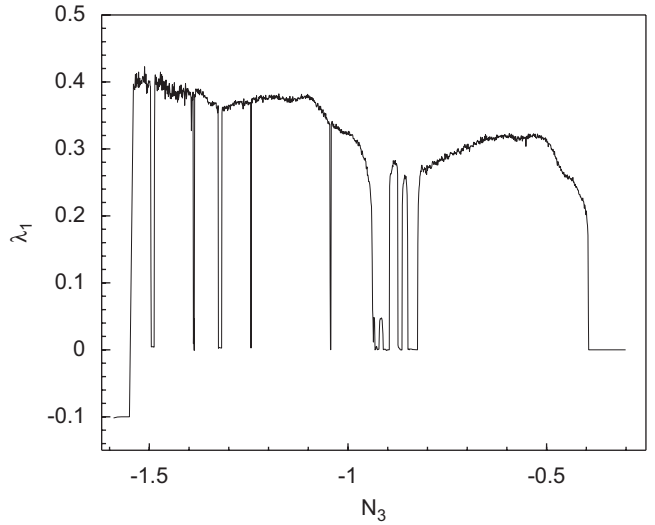

Fig. 10. Dependence of the maximum Lyapunov exponent λ_1 on N_3.

structure and look as a chaotic point set. Any one-dimensional approximation of Poincaré map is impossible (Fig. 9(d)) Developed chaotic attractors, as shown in Fig. 9, are the most typical for system (20). They exist at the dominant majority of values N_1 from a segment $[-0.373, -0.10165]$.

Let us consider now bifurcations which happen in system (20), when the static characteristic of the electromotor is changing by the value of N_3 (multiparameter, which depends on the eigenfrequency of fluid free surface and on characteristics the electromotor). We assume that $N_1 = -1$, and values A, B, α, μ_1 remain the same, as in Eqs. (22)–(24). In Fig. 10 dependence of the maximum Lyapunov characteristic exponent λ_1 on value N_3 is shown. The graph in Fig. 10 displays that at $-1.6 < N_3 < -0.394$ there are some intervals in which the exponent λ_1 is positive. Hence, in these intervals the system of equations (20) has chaotic attractors. Apparently from Fig. 10, intervals in which there are chaotic attractors, alternate with narrow "windows" of periodicity.

Let us study some features of transition to chaos at changing of the bifurcation parameter N_3. So, at $N_3 = -0.38$ in the system there is a stable limit cycle. At decreasing of values N_3 an infinite cascade of bifurcations of period-doubling starts and comes to an end by origin of a chaotic attractor at $N_3 \approx -0.395$. The arisen chaotic attractor exists in very small interval of N_3 and it is replaced by a chaotic attractor of other type already at $N_3 = -0.39504$ as a result of an intermittency. The newly arisen chaotic attractor exists in the larger interval of N_3, namely, $-0.5 < N_3 \leqslant -0.39504$. Such a situation reminds one of what was considered earlier in the study of bifurcations on parameter N_1 at the right threshold of existence of chaos. However, in the latter case there is one essential difference: the limit cycles originating under Feigenbaum scenario a chaotic attractor are not single-mode ones. They have oscillations by both dominant modes.

In Fig. 11(a) and (b) projections of phase portraits of chaotic attractors are constructed at $N_3 = -0.39503$ and -0.39504 accordingly. A chaotic attractor, shown in Fig. 11(b), differs from a chaotic attractor, given in Fig. 11(a), by noticeable growth of vibration amplitudes on both dominant modes. It courses an essential growth of an area in the phase space in which the arisen attractor is localized. In Fig. 11(c) and (d) the projections of phase portraits of chaotic attractors in a larger scale are shown. As it is well seen from these figures, the fragment of the projection of the chaotic attractor at $N_3 = -0.39504$ is qualitatively similar to the chaotic attractor at $N_3 = -0.39503$. These graphs make clear the mechanism of an intermittency at origin of one attractor from another. In the point of the bifurcation the chaotic attractor in Fig. 11(a) disappears and in system (20) an attractor of new type appears, trajectory motion on which will consist of two phases. One of them whom, as well as earlier, we shall name coarse grained laminar, represent chaotic wanderings along a trajectory of the arisen attractor in neighborhoods of trajectories of the missed chaotic attractor. At an unpredictable instant of time the trajectory "becomes broken" and a moving point goes away from the area of

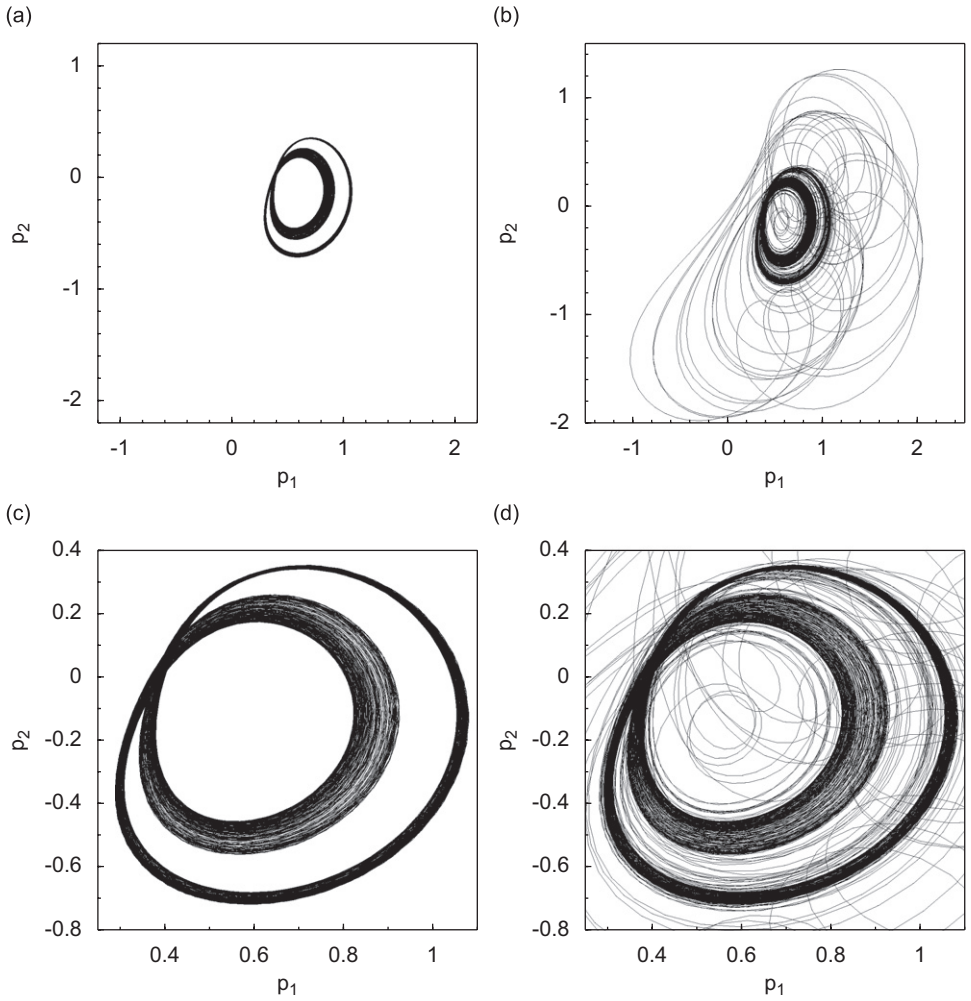

Fig. 11. Projections of chaotic attractor phase portraits at $N_3 = -0.39503$ (a,c) and at $N_3 = -0.39504$ (b,d).

the missed chaotic attractor to far fields of the phase space. It is a turbulent phase of motion along the trajectory. Then the trajectory again returns in the area of the missed attractor. This process iterates an infinite number of times.

In Fig. 12(a) and (b) projections of distribution of an invariant measure in phase portraits are shown for the chaotic attractors at $N_3 = -0.39503$ (Fig. 12(a)) and at $N_3 = -0.39504$ (Fig. 12(b)). In Fig. 12 densely blacked out parts correspond to coarse grained laminar phase of an intermittency and more light to turbulent splashes. From this figure it could be clearly seen that duration of the coarse grained laminar phase considerably exceeds duration of the turbulent phase. Distribution of an invariant measure in the phase portrait of the chaotic attractor in Fig. 12(a) is uniform enough, what is typical for chaotic attractors, arisen under Feigenbaum scenario. The qualitative similarity between Fig. 12(a) and (b) here is well visible and indicates that the vanishing chaotic attractor serves as a "foundation" for the coarse grained laminar phase of the originating attractor.

In Fig. 12(c) and (d) Poincaré sections by the plane $\beta = -0.5$ of these attractors are shown. Both Poincaré sections are dot chaotic sets. One of the sections (Fig. 12(d)) as a fragment contains a set qualitatively similar to the second section (Fig. 12(c)) that once again confirms the presence of the intermittency of new type "chaos–chaos" in the system. Thus, there is the intermittency which is distinct from classical Pomeau–Manneville scenarios [21–23].

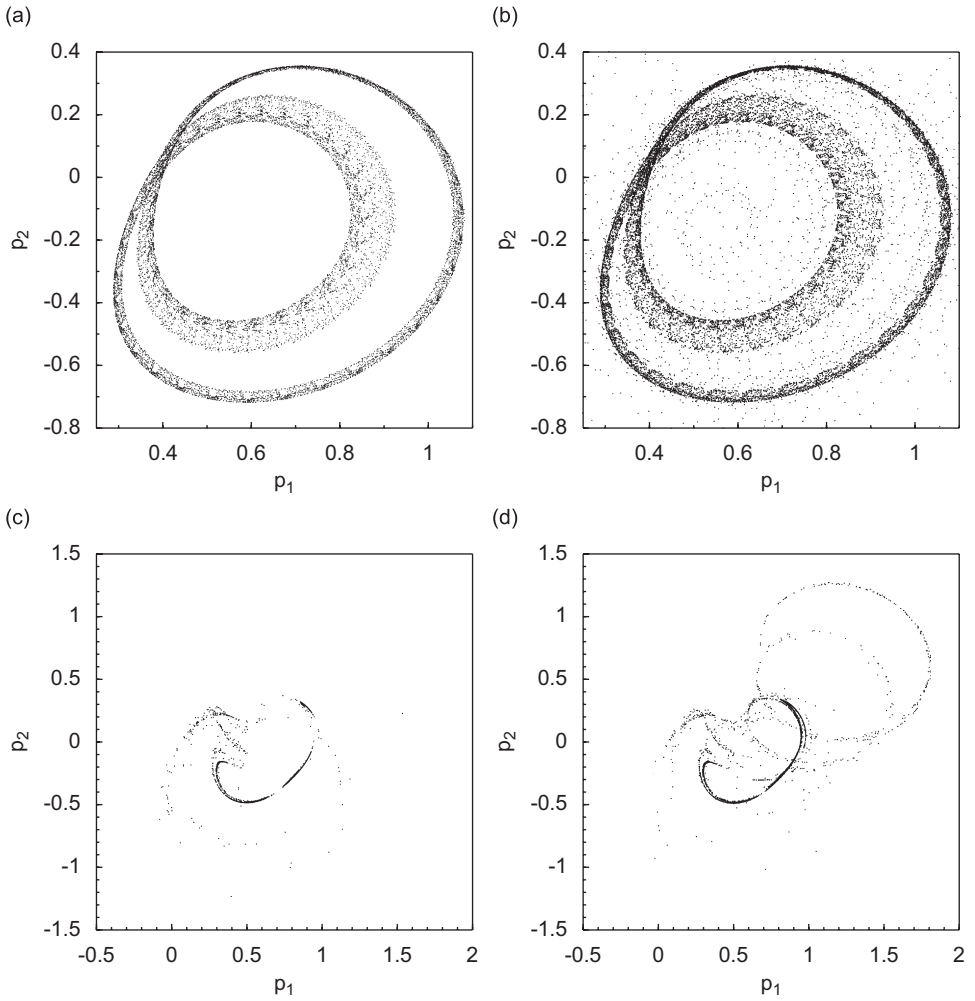

Fig. 12. Projections of distributions of an invariant measure and sections of Poincaré of chaotic attractors at $N_3 = -0.39503$ (a,c) and at $N_3 = -0.39504$ (b,d).

Now we consider the behavior of the system when parameter N_3 is passing through a window of periodicity in more detail. For that we assume that $N_3 \in [-0.828, -0.825]$. A limit cycle is as an attractor of the system in this window of periodicity. In Fig. 13(a) and (b) projections of a phase portrait and Poincaré section of the cycle are constructed at $N_3 = -0.825$, accordingly. The structures of graphs are typical for limit cycles, namely: a closure of a trajectory in a phase space and finiteness of points in Poincaré section. At small increasing of N_3 system (20) instead of the limit cycle has a chaotic attractor. Projections of a phase portrait and distribution of Krylov–Bogolyubov invariant measure on a phase portrait of the new chaotic attractor, constructed at $N_3 = -0.824$, are given in Fig. 13(c) and (d). The last figure is a good illustration of transition history from the regular attractor to a chaotic one. An area densely retraced is practically coincident with the missed limit cycle, as we can see in Fig. 13(d) clearly. It is a laminar phase of an intermittency "a limit cycle–chaos". The lighter parts of the graph characterize a turbulent phase of this intermittency.

In Fig. 14 (a) and (b) projection of Poincaré section by the plane $\beta = -1.35$ and Poincaré map of a chaotic attractor at $N_3 = -0.824$ are given. Both represent developed chaotic point sets. The arisen chaotic attractor is a double-mode one. Such type of attractors are the most typical for system (20). They exist for the majority of values N_3 of chaos field, found using analysis of Fig. 10. In particular, chaotic attractors of such type exist at the left-hand boundary of the chaotic field in Fig. 10. At decreasing of N_3 at this boundary ($N_3 \approx -1.544505$) the chaotic attractor disappears and a position of an equilibrium with $p_1 = \text{const.}$, $q_1 = \text{const.}$, $\beta = \text{const.}$,

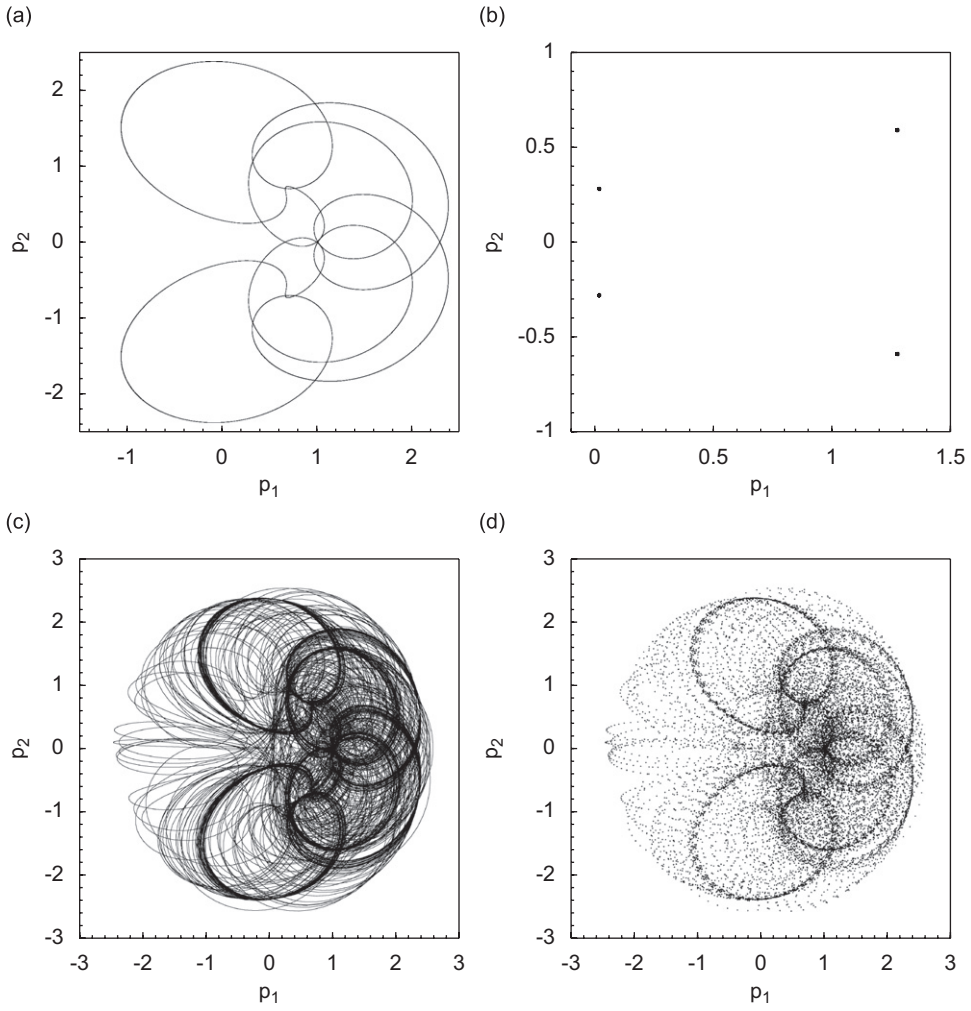

Fig. 13. Projections of a phase portrait and Poincaré section of a limit cycle at $N_3 = -0.825$ (a,b); projections of a phase portrait and distribution of an invariant measure of a chaotic attractor at $N_3 = -0.824$ (c,d).

$p_2 = q_2 = 0$ establishes in the system. The characteristic for such position of an equilibrium is the equality to zero of the second dominant mode variables. So, for $N_3 = -1.544506$ the position of an equilibrium has the following coordinates:

$$p_1 = 0.84, \quad q_1 = 0.07, \quad \beta = -1.58, \quad p_2 = q_2 = 0. \tag{26}$$

In conclusion we consider bifurcations of system (20) which happen at the changing of the parameter α (coefficient of damping). We assume that $N_1 = N_3 = -1$, and values A, B, μ_1 are the same, as in Eqs. (22) and (24). In Fig. 15 dependence of the maximum Lyapunov characteristic exponent λ_1 on the coefficient of damping α is shown. In that figure intervals of a positiveness of the characteristic exponent are precisely visible. In these intervals the system has chaotic attractors. As well as in the previous cases, intervals of a chaos alternate with very small intervals, in which the maximum characteristic exponent is equal to zero. These are windows of periodicity in chaos, in which attractors of system (20) are limit cycles.

There is a stable limit cycle at $\alpha = -0.3115$. At increase α, starting from $\alpha = -0.311$, the infinite cascade of period-doubling bifurcations realizes which ends by origin of a chaotic attractor at $\alpha \approx -0.3109$. A rule typical enough for this problem is again observed: transition to chaos under the scenario Feigenbaum is implemented in very small interval $(-0.311, -0.3109)$. In Fig. 16(a)–(c) the first bifurcations of a period–doubling cascade

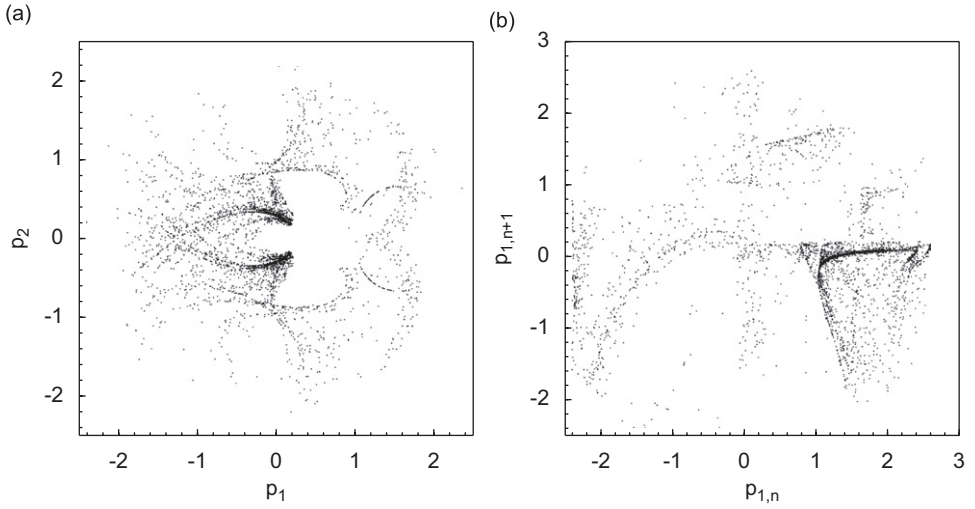

Fig. 14. Projections of Poincaré section and map of a chaotic attractor at $N_3 = -0.824$ (a,b).

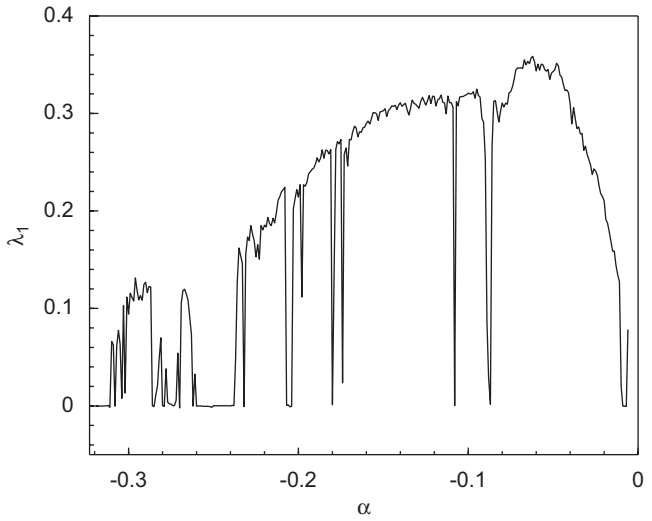

Fig. 15. Dependence of the maximum Lyapunov exponent λ_1 on α.

are shown. And in Fig. 16(d) chaotic attractor projections that have arisen by the Feigenbaum scenario are shown. Chaotic attractors of this type (Fig. 16(d)) have a ribbon structure of its Poincaré section.

The described scenario of transition to chaos iterates at passing α right boundary of a window of periodicity. Everywhere the cascade of period-doubling bifurcations happen in very small interval changes of parameter. As a result of bifurcations chaotic attractors appear which look as is shown in Fig. 16(d). Further on in all intervals of a chaos the following regularity takes place. At moving α from the right boundary of a periodicity window a chaotic attractor becomes more "developed". Its trajectories start to fill in all hollows which can be seen in Fig. 17(a) and (b). At the same time Poincaré sections lose ribbon structure and look like chaotic point sets, Fig. 17 as illustration serves. In this figure different characteristics of a chaotic attractor are given which are constructed at $\alpha = -0.15$, which is approximately in the middle of this interval of chaos (see Fig. 15).

Let us notice that the structure of a phase portrait of a chaotic attractor on the last figure is the most typical for chaotic attractors which exist in system (20). Practically always, attractors have a similar phase portrait at chaos in a case when the bifurcation parameter is in some distance from periodicity window boundaries. However, resembling of phase portraits does not entail resembling Poincaré sections and maps. Really, the

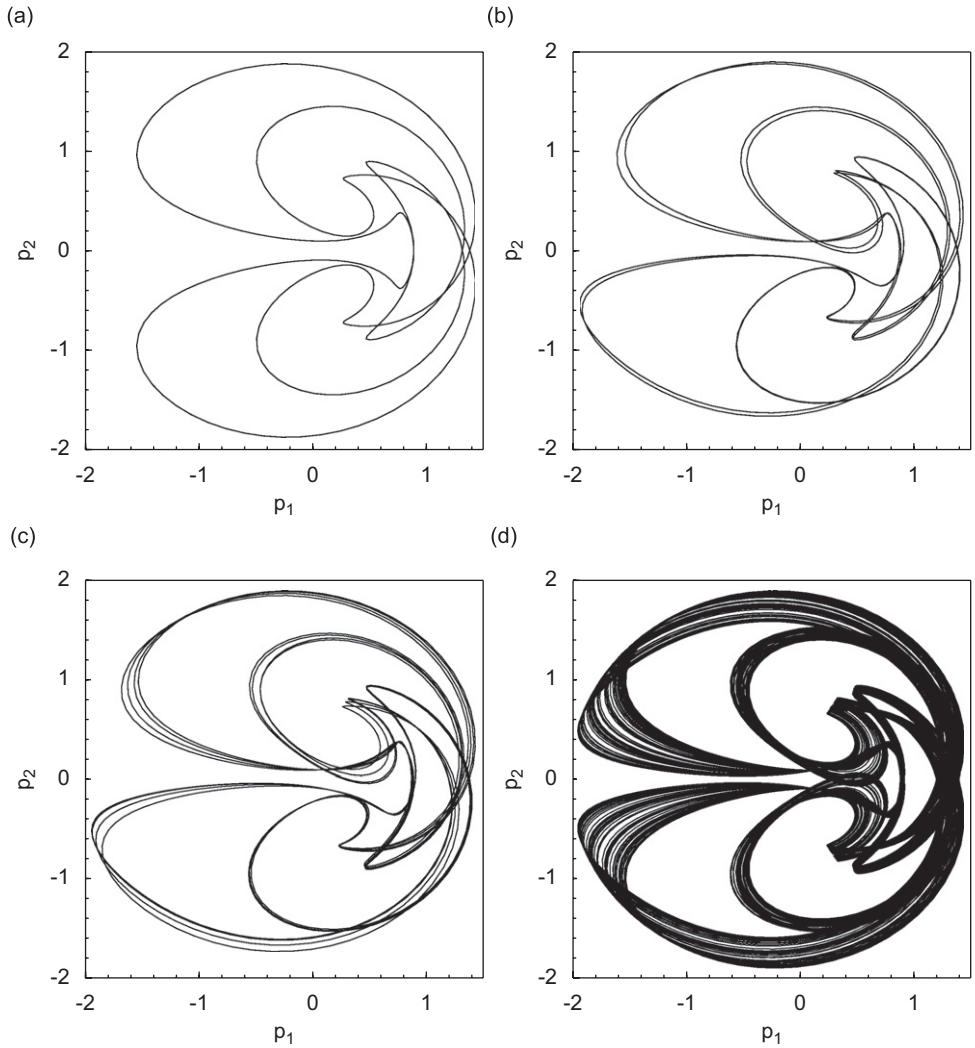

Fig. 16. Projections of a period—doubling bifurcation cascade (a)–(c) and projection of chaotic attractors at $\alpha = -0.31084$ (d).

chaotic attractor constructed at $\alpha = -0.188$ (as it is clear from Fig. 15 this value α, as well as $\alpha = -0.15$ is far enough from periodicity window boundaries) has projections of phase portrait practically indistinguishable from the relevant projections of a chaotic attractor at $\alpha = -0.15$. Therefore, we do not show these projections here. For a visual image of a phase portrait of a chaotic attractor at $\alpha = -0.188$ it is enough to look at Fig. 17(a) and (b). Poincaré sections (by the same intersecting plane $\beta = -1.55$) and maps of attractors at $\alpha = -0.15$ and -0.188 differ from each other very much. So, in Fig. 18(a) and (b) projections of Poincaré section by the plane $\beta = -1.55$ and map of the variable q_2 (c) and (d) of the chaotic attractors are shown. Comparison the relevant parts of Figs. 17 and 18 displays the considerable differences in structure of Poincaré sections and maps of two considered chaotic attractors. Sections and maps represent developed chaotic sets for both attractors. Approximation of such sets by the one-dimensional curves is impossible.

The carried out numerical calculations have shown that in the space of parameters of system (20) a three-dimensional range of parameters N_1, N_3, α can be localized in which chaotic attractors are more typical attractors of the investigated system than the regular attractors. Really, we mark as Pr a three-dimensional parallelepiped in space of parameters of system (20) whose boundaries are determined by requirements:

$$-0.32 < \alpha < 0, \quad -0.4 < N_1 < -0.1, \quad -1.6 < N_3 < -0.35,$$

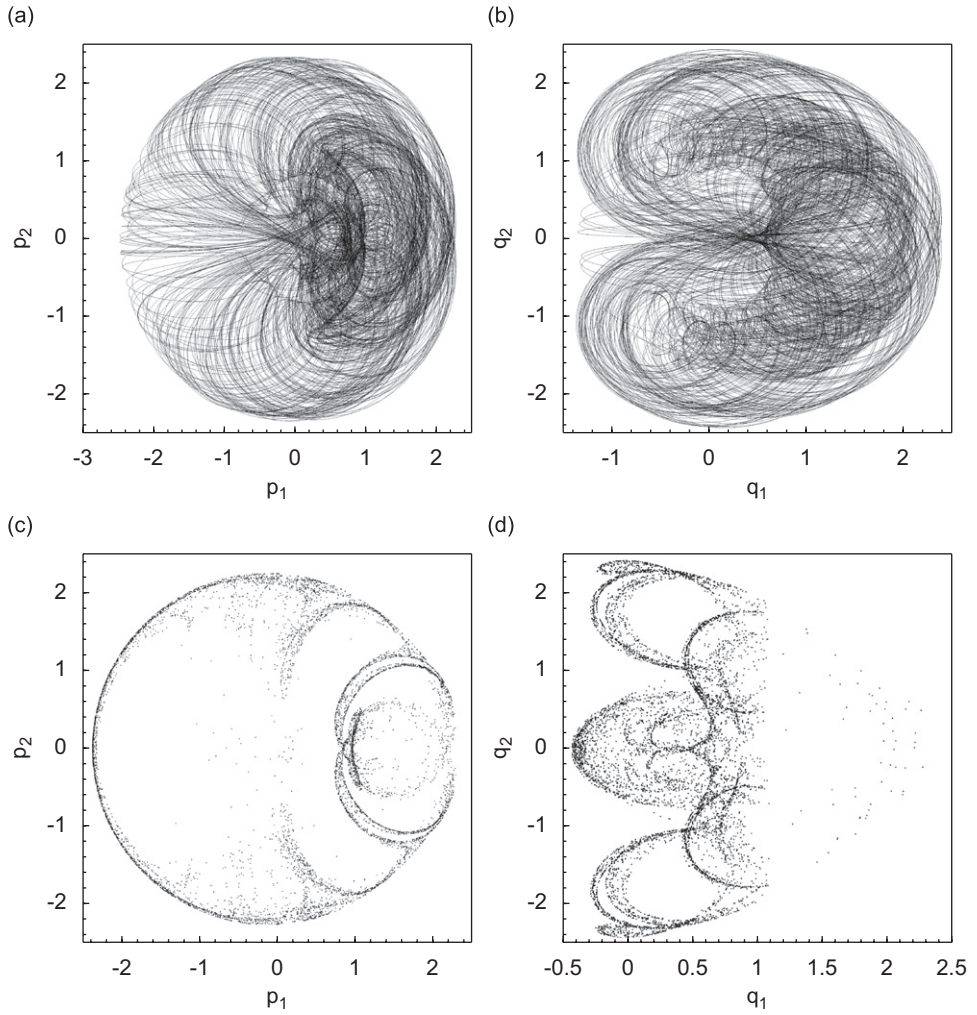

Fig. 17. Projections of a phase portrait (a,b) and projections of Poincaré section (c,d) of the chaotic attractor at $\alpha = -0.15$.

$$A = 1.112, \quad B = -1.531, \quad \mu_1 = 0.5. \tag{27}$$

Practically, for all values of parameters of system (20) which are inside *Pr* a unique possible attractor in the vicinity of an origin of coordinates is the chaotic attractor.

Let us assume that the range of initial conditions is defined by the following relations:

$$|p_i| \leqslant 2.5, \quad |q_i| \leqslant 2.5, \quad |\beta| \leqslant 2.5, \quad i = 1, 2. \tag{28}$$

Satisfying in our numerical experiments requirements (27) and (28) it was possible to define a two-parameter region *Ca* whose boundaries are approximately as follows:

$$-1.5N_1 - 0.05 \leqslant N_3 \leqslant -0.475N_1 + 0.08, \quad 0 < N_1 \leqslant 10. \tag{29}$$

In limits of the region *Ca* small "islands" exist whose total area is much less than the area of *Ca*. In these islands the only possible attractors of system (20) are regular ones. For all remaining values $N_1, N_3 \in Ca$ unique existing attractors of the dynamic system (20) are chaotic attractors of considered types. And the single-mode attractors can exist only in very narrow bands located along boundary *Ca*. Transition from the regular to chaotic motion happens under the earlier described scenarios, including the new "non-classical" scenario of intermittency.

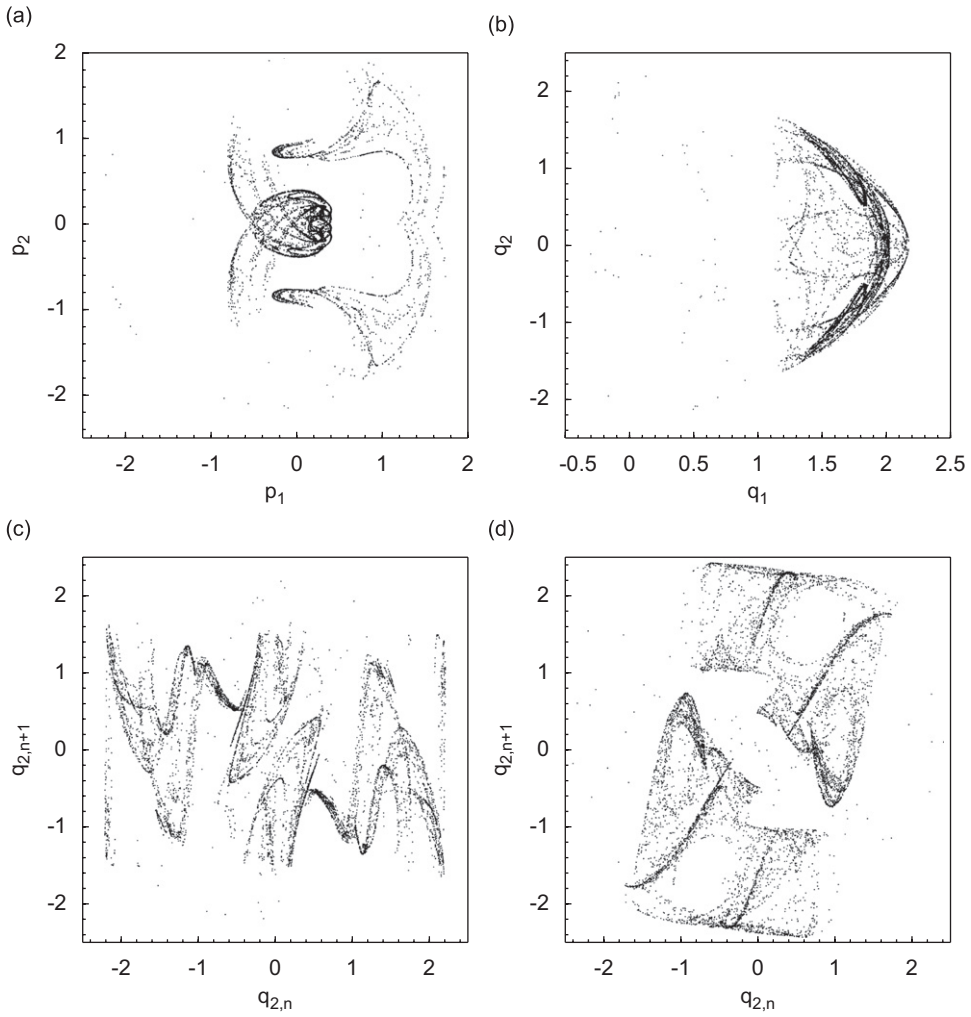

Fig. 18. Projections of Poincaré sections (a), (b) and map (c) of the chaotic attractor at $\alpha = -0.188$; map of (d) of the chaotic attractor at $\alpha = -0.15$.

Returning to the real physical system: the tank with fluid free surface and the electric motor, we should notice the following. We have shown that the chaotic regimes of resonant fluid forced oscillations are quite different when the interaction with the excitation source is taken into account. The differences are mainly due to the fact that interaction in most cases leads to a non-constant frequency β (''detuning''). β will be constant (although not equal to the initial value of β_0) only at the equilibrium positions of system (20). In other steady-state regimes of interaction the value of β changes in some regions (since the speed $\dot{\Theta}(t)$ depends on fluid vibrations and also changes in some interval of value). Moreover, these changes will be periodic or chaotic, respectively, for periodic or chaotic regimes of system (20). Thus, for a certain initial value of the frequency detuning β_0 will eventually trace the whole interval of values of β. The changing of β does not allow a direct comparison of the resonance curves under ideal (unlimited power supply) and non-ideal (limited power supply) excitation. The frequency detuning in the case of non-ideal excitation will be a function of $\beta_0, p_1, q_1, p_2, q_2$ and τ.

In summary, the observed steady-state solutions of system correspond to the following three main classes of steady-state regimes of real physical ''fluid-energy source'' system: the first class includes regular regimes which correspond to equilibrium positions of the system, when fluid vibrations in the resonance modes occur with constant amplitude and frequency, and the electric motor shaft rotates with constant velocity. The second

class includes regular regimes which correspond to limit cycles of system (20), and in which vibrations of the dominant modes have periodically changing amplitude and frequency, the shaft rotates with the speed which has periodically changing component. The third class corresponds to chaotic attractors of system (20) when the amplitude and frequency of fluid vibrations and the electric motor velocity change chaotically in time. The third class of regimes differs qualitatively from the other two and cannot be approximated by them.

4. Conclusion

As a result of investigating the nonlinear process of interaction between the resonant vibrations of a fluid free surface in the cylindrical tank and the electric motor with limited power supply the following conclusions can be drawn.

The existence of several types of chaotic attractors was established for the described system. It was shown that the transition to chaotic motion may occur with different scenarios such as: a cascade of period-doubling bifurcations, the intermittency by classical Pomeau–Manneville scenario and the intermittency of new type "chaos–chaos" which generalizes the previous one.

It was shown that the chaotic steady regimes are typical attractors for the described system. In the parameters space, large regions were found where chaotic motions exist.

It was established for averaged systems that chaos could originate only from the process of interaction of a directly excited resonance mode of vibrations with the electric motor during forced resonance, when a second dominant mode was not excited altogether. One-mode chaotic regimes could not occur in the case of an ideal excitation.

References

[1] J.W. Miles, Internally resonant surface waves in circular cylinder, *Journal of Fluid Mechanics* 149 (1984) 1–14.
[2] J.W. Miles, Resonantly forced surface waves in circular cylinder, *Journal of Fluid Mechanics* 149 (1984) 15–31.
[3] M. Amabili, M.P. Païdoussis, A.A. Lakis, Vibrations of partially filled cylindrical tanks with ring-stiffeners and flexible bottom, *Journal of Sound and Vibrations* 213 (2) (1998) 259–299.
[4] R.A. Ibrahim, *Liquid Sloshing Dynamics: Theory and Applications*, Cambridge University Press, Cambridge, 2005 956pp.
[5] T.S. Krasnopolskaya, A.Yu. Shvets, Regular and chaotic dynamics of systems with limited excitation, RCD, Moskow-Izhevsk, 2008, 280pp (in Russian).
[6] V.O. Kononenko, *Vibrating System with a Limited Power-supply*, Iliffe, London, 1969 236pp.
[7] A. Sommerfeld, Beitrage zum dynamischen Ausbau der Festigkeitslehre, *Zeitschrift des Vereines deutscher Ingenieure* 46 (1902) 391–394.
[8] S. Timoshenko, *Vibration Problems in Engineering*, Van Nostrand Co, New York, 1928 480pp.
[9] T.S. Krasnopolskaya, A.Yu. Shvets, Chaotic surface waves in limited power-supply cylindrical tank vibrations, *Journal of Fluids and Structures* 8 (1) (1994) 1–18.
[10] T.S. Krasnopolskaya, A.Yu. Shvets, Chaotic interaction between fluid vibrations in a cylindrical tank and electromotor, *Flow Induced Vibration*, A.A. Balkema, Brookfield, Rotterdam, 1995, pp. 269–280.
[11] J.W. Miles, Nonlinear surface waves in closed basins, *Journal of Fluid Mechanics* 75 (1976) 419–448.
[12] J.H. Dormand, P.J. Prince, A family of embedded Runge formulae, *Journal of Computational Applied Mathematics* 6 (1980) 19–27.
[13] M. Henon, On the numerical computation of Poincaré maps, *Physica D* 5 (2) (1982) 412–415.
[14] G. Benettin, L. Galgani, J.M. Strelcyn, Kolmogorov entropy and numerical experiments, *Physics Review A* 14 (6) (1976) 2338–2342.
[15] G. Benettin, L. Galgani, A. Giorgilli, J.M. Strelcyn, Lyapunov characteristic exponents for smooth dynamical systems and for Hamiltonian systems; a method for computing all of them. P.1, *Meccanica* 15 (1) (1980) 9–20.
[16] M.J. Feigenbaum, Quantitative universality for a class of nonlinear transformations, *Journal of Statistical Physics* 19 (1) (1978) 25–52.
[17] M.J. Feigenbaum, The universal metric properties of nonlinear transformations, *Journal of Statistical Physics* 21 (6) (1979) 669–706.
[18] J.W. Gibbs, *Elementary Principles in Statistical Mechanics*, Scribner, NewHaven, 1902 584pp.
[19] T.S. Krasnopolskaya, V.V. Meleshko, G.W.M. Peters, H.E.H. Meijer, Mixing in Stokes flow in an annular wedge cavity, *European Journal of Mechanics, B—Fluids* 18 (1999) 793–822.
[20] V.V. Meleshko, T.S. Krasnopolskaya, Stirring of viscous fluids, *Nonlinear Dynamics* 1 (1) (2005) 69–109 (in Russian).
[21] P. Berge, Y. Pomeau, C.H. Vidal, *Order within Chaos*, Wiley, New York, 1984 368pp.
[22] Y. Pomeau, P. Manneville, Intermittent transition to turbulence in dissipative dynamical systems, *Communications in Mathematical Physics* 74 (2) (1980) 189–197.
[23] A.Yu. Shvets, Scenarios of transitions "order–chaos" at resonant vibrations of fluid in cylindrical tanks, *Proceedings of Institute of Mathematics NASU* 3 (1) (2006) 216–249 (in Russian).